EAST EUROPEAN JOURNAL OF PHYSICS. 3. 269-279 (2026)
DOI:10.26565/2312-4334-2026-3-21 ISSN 2312-4334

THERMODYNAMIC AND EXERGY ANALYSIS OF AN AP1000-BASED STEAM TURBINE UNIT WITH OPTIMIZED CYCLE CONFIGURATION

Andrii V. Rusanov[1], Andrii O. Kostikov[1], Viktoriia O. Tarasova[1]*, Roman A. Rusanov[1], Marina O. Chugay[1], Maksym V. Lytvynenko[2]

[1]*A. Pidhornyi Institute of Power Machines and Systems of the NAS of Ukraine, Komunalnykiv 2/10 str., Kharkiv, 61046, Ukraine*
[2]*Institute of Fluid-Flow Machinery Polish Academy of Sciences, Fiszera 14 st. Gdańsk 80-231, Poland*
**Corresponding Author e-mail: vat523710@gmail.com*
Received May 22, 2026; revised July 30, 2026; accepted August 21, 2026

Given the strategic importance of Ukraine's nuclear energy sector modernization, the paper presents the results of the investigation into the development and analysis of the cycle configuration of a steam turbine unit (STU) intended for operation with the AP1000 nuclear reactor. The K-1000-60/1500-2 turbine unit was selected as the reference configuration. Based on this design, a new cycle configuration was proposed that includes a combined single-flow high- and intermediate-pressure turbine (HIPT), two low-pressure turbines (LPTs), a steam separator, and a two-stage steam reheating system. A thermodynamic and exergy analysis of the proposed STU configurations was performed to evaluate the influence of steam extraction pressures, regenerative feedwater heating parameters, and turbine stage distribution on the cycle performance. Numerical simulations and flow-path calculations of the turbine sections were performed using modern gas-dynamic design methods. The results show that the optimal selection of steam extraction parameters and intermediate reheating conditions significantly improves the cycle efficiency. The maximum internal efficiency of the STU cycle reached 38.96 %. Exergy analysis demonstrated that the largest exergy destruction occurs in the low-pressure turbine section, while both investigated configurations exhibit high exergy efficiency. A comparative analysis of the turbine stage configurations and the axial dimensions of the turbine flow parts was also conducted. The developed approaches can be applied in the design and optimization of next-generation steam turbine units for nuclear power plants.
Keywords: *Nuclear energy; AP1000; Steam turbine unit; Thermodynamic analysis; Exergy analysis; Regenerative feedwater heating; Nuclear power plant*

1. INTRODUCTION

Nuclear energy is a fundamental component of Ukraine's energy security and one of the most important factors in long-term decarbonization, particularly amid wartime destruction and the loss of a significant share of heat and power generation capacity. Since 2022, the demand for reliable baseload electricity sources in Ukraine has increased substantially, making Generation III+ nuclear units a priority direction for development.

The AP1000 nuclear reactor, developed by Westinghouse Electric Company, is one of the most advanced pressurized water reactors (PWRs), with a thermal output of 3415 MW and an electrical output of 1117–1200 MW [1–3]. It is characterized by passive safety systems and high operational performance. Therefore, the AP1000 appears to be promising for deployment at Ukrainian nuclear power plants (NPPs), including the Khmelnitsky NPP [4].

However, integrating the AP1000 requires developing an optimized cycle configuration for the steam turbine unit (STU) that fully matches the parameters of the saturated steam produced in the steam generator. Existing cycle configurations designed for VVER-1000 units do not fully utilize the thermodynamic potential of the AP1000, necessitating the modeling and implementation of new engineering solutions [5–7].

Therefore, the development and analysis of an STU cycle configuration for the AP1000, aimed at improving the efficiency through the optimal distribution of extraction pressures, is a relevant and practically significant research task.

2. LITERATURE REVIEW ON THE AP1000

The current scientific literature on Generation III+ reactors focuses on the AP1000 model, which is one of the most widely used in the global nuclear energy industry. Several key sources can be identified to cover the design, characteristics, and operation of AP1000 reactors. Papers [2–3] show the basic technical characteristics of the reactor, including a thermal power of 3415 MW, an electrical power of over 1100 MW, core parameters, and a detailed description of the passive safety systems. This material is fundamental, as it contains the official nominal parameters, a diagram of the steam generators, a description of the primary cooling system, as well as safety systems.

The report [8] provides an independent expert assessment of the project. It focuses on the reliability of the safety systems, the behavior of the core under emergency conditions, and the design's compliance with international requirements. The document provides a detailed overview of the reactor plant, steam generators, and the emergency heat exchange system, making it one of the most valuable sources for analyzing the AP1000 engineering design.

Cite as: A.V. Rusanov, A.O. Kostikov, V.O. Tarasova, R.A. Rusanov, M.O. Chugay, M.V. Lytvynenko, East Eur. J. Phys. 3, 269 (2026), https://doi.org/10.26565/2312-4334-2026-3-21

The research paper [9] reveals key features of the commercial operation of the AP1000 reactor at the Sanmen NPP in China. Such key issues as the reliability of passive safety systems, scalability, and verification and validation experiments needed to improve the safety of the AP1000, are discussed in the paper.

A thermal and hydraulic analysis of the AP1000 reactor vessel under nominal operating conditions using a 3D CFD model is presented in paper [10]. The AP1000 Advanced Nuclear Reactor (NR) stands out among other PWRs in terms of generation technology due to its innovative features of reliability, modularity and, most importantly, passive safety systems.

In the study [11], an assessment of the possibilities of deploying AP1000 reactors at existing and new sites was carried out. The document contains technical and economic aspects, including a comparison of implementation options, impact on energy infrastructure, and cost parameters. This source is important in the context of strategic planning for the introduction of AP1000 into state power systems.

Also, the leading areas of research are neutron-physical analysis, core safety indicators and the operation of reactivity control systems, described in papers [12 – 15]. So, the paper [12] shows the influence of fuel temperature, moderator density, boron concentration and control rod condition for AP1000 reactor on the safety parameters.

Thus, the analyzed literature demonstrates that AP1000 is mainly studied in three areas:

– design and passive safety systems [1 – 3, 5, 9, 10];

– neutron and thermal hydraulic analysis of the reactor [12 – 15];

– economic and strategic aspects of implementation [11].

These sources form a complete picture of the capabilities of the AP1000, its design features, safety and implementation prospects.

In contrast to the significant number of papers on design review and neutron-physical analysis, the literature that considers the cycle configuration of a steam turbine plant of a nuclear power plant with the AP1000 nuclear reactor is much less common.

In [16], a system that is designed for reliable and efficient storage and recovery of thermal energy from the steam system of a nuclear power plant (NPP) to ensure flexible electricity production using an economical and scalable design is presented. In [17], the role of energy storage technologies in their integration into NPPs is assessed.

In papers [18 – 20], combined cycles are proposed to increase the efficiency of NPP power units, in particular with gas turbines and hydrogen combustors.

All these measures [16 – 20] significantly increase the output power and efficiency of NPPs. But they are also associated with special safety conditions and require additional research before their implementation into existing NPPs.

Therefore, the problem of increasing the efficiency of a steam turbine unit through thermodynamic analysis and exergy optimization of the cycle, as well as improving the steam turbine flow path using 3D design and modeling [21 – 22] remains relevant.

3. AIM AND OBJECTIVES OF THE STUDY

The aim of the paper is to develop and analyze the cycle configuration of a steam turbine unit intended for operation with the AP1000 nuclear reactor, as well as to determine optimal steam extraction parameters and turbine stage configurations that ensure high thermodynamic and exergy efficiency of the cycle.

To achieve this goal, the following objectives were formulated:

1 To analyze existing condensing steam turbine units of nuclear power plants and select a baseline turbine configuration suitable for adaptation to operation with the AP1000 reactor, taking into account the parameters of saturated steam.

2 To develop a new cycle configuration of the steam turbine unit with a combined high- and intermediate-pressure turbine, regenerative feedwater heating system, steam separator, and intermediate steam reheating.

3 To perform thermodynamic modeling of the AP1000-based steam turbine unit and determine optimal steam extraction pressures that provide maximum cycle efficiency.

4 To develop and compare several options of the turbine flow part configuration with different numbers of turbine stages and steam extraction arrangements.

5 To carry out an exergy analysis of the proposed cycle configuration, including determination of exergy destruction and exergy efficiency of the main elements of the steam turbine unit using the fuel–product approach.

6 To analyze the geometric characteristics of the turbine flow parts and evaluate the influence of turbine stage distribution on the axial dimensions of the steam turbine unit.

4. DEVELOPMENT OF THE CYCLE CONFIGURATION OF AN AP1000-BASED STEAM TURBINE UNIT

4.1. OVERVIEW OF CONDENSING-TYPE STEAM TURBINES OF NUCLEAR POWER PLANT UNITS

Several models of low-speed condensing-type steam turbines K-1000-60/1500, developed by the Joint-Stock Company "Ukrainian Power Machines", are implemented on nuclear power plant units with VVER-1000 reactors. The

K-1000-60/1500 turbine has several modifications. The K-1000-60/1500-1 has a capacity of 1030 MW. The turbine unit is 57.4 m long (50.7 m without the generator), contains one high-pressure turbine (HPT), one intermediate-pressure turbine (IPT) and three low-pressure turbines (LPT). It is equipped with side single-flow condensers. A turbine of the STU K-1000-60/1500-2 has a reduced length of up to 52.2 m. The total mass is reduced by 350 tons. For the cycle configuration developing, the K-1000-60/1500-2 steam turbine unit was taken as a basis [6, 7]. This turbine unit is designed for a nuclear power plant with an electric power of 1200 MW at 3000 rpm. K-1000-60/1500-2 steam turbine unit is intended to operate in a monoblock with an AP1000 PWR with a thermal power of 3400 MW on saturated steam.

4.2. DEVELOPMENT OF A CYCLE CONFIGURATION OF A STU WITH AP1000 REACTOR

A new STU cycle configuration with a combined HIPT is proposed. Unlike the K-1000-60/1500-2 STU, the new configuration includes a single-flow HIPT, two LPTs, and two condensers instead of the three LPTs and three condensers used in the K-1000-60/1500-2 (Fig. 1).

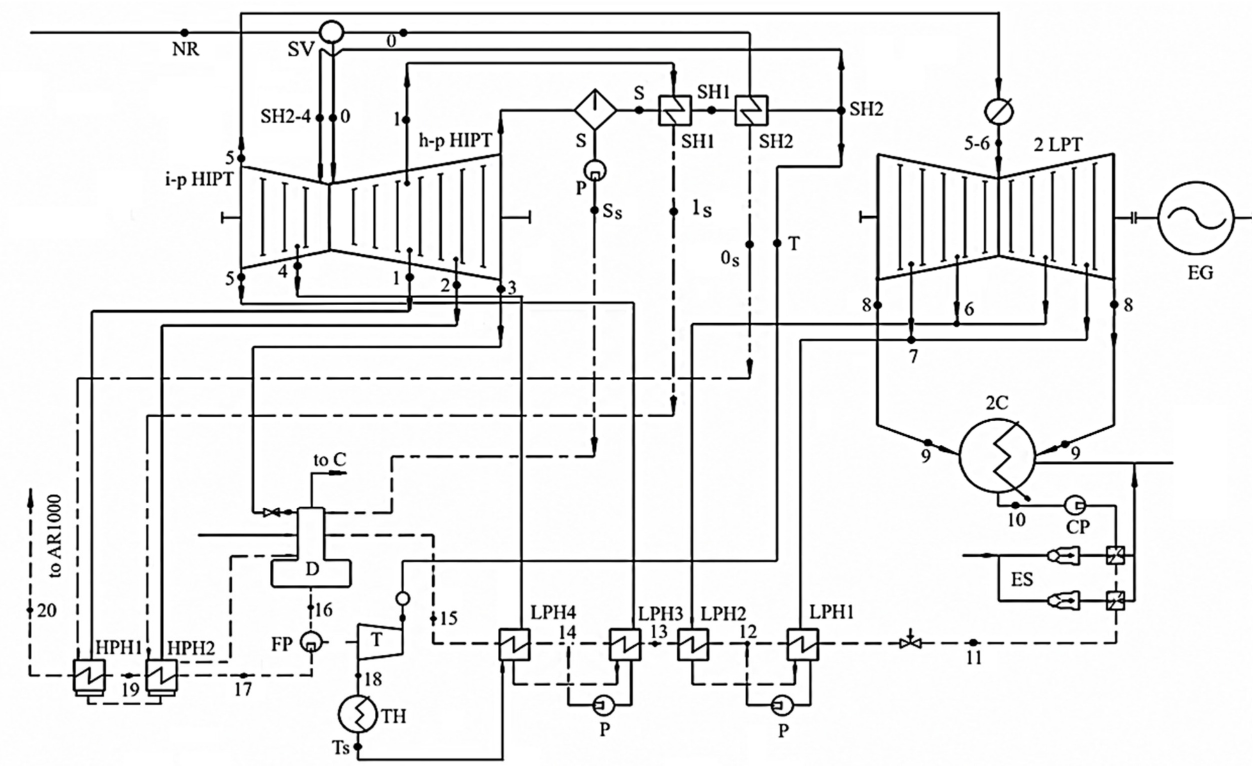

Figure 1. Cycle configuration of a steam turbine unit with AP1000
P– pump; SV – steam stop valve; ES – ejector system; T – turbine; TH – heater; EG – electric generator

The scheme includes a single separation and two-stage reheating of steam. In this case, fresh steam is supplied to the high-pressure part of the HIPT (h-p HIPT). After reaching the permissible humidity, the steam is directed to the external separator (S), where it is dried. After drying and superheating in the superheaters (SHs), the steam enters the intermediate-pressure turbine part (i-p HIPT), and then is directed towards two LPTs. Next, the exhaust steam is directed to the two condensers (C), and then the condensate – to the regeneration system. In the second SH, the steam is reheated by a fresh steam. The main condensate is pumped from the C to the deaerator (D) by condensate pumps (CP). The feed water from the deaerator through the high-pressure heater (HPH) to the steam generator is supplied by a feed pump (FP) with an electric drive.

Pressure losses during steam throttling in the turbine control elements are assumed to be 5%. Pressure losses of 5% are also taken into account in the steam lines leading to the HPHs and low-pressure heaters (LPH).

The initial data for calculating the cycle configuration of a steam turbine unit with the AP1000 reactor:

Steam mass flow rate per turbine – 1878 kg/s;

Absolute fresh steam pressure – 5.877 MPa;

Fresh steam temperature – 274.3 °C;

Absolute condenser pressure – 5 kPa;

Feed water temperature – 226.8 °C.

The distribution pressure at the outlet of the high-pressure part of HIPT is $P_3 = 1.1331$ MPa, and the saturation temperature at this pressure is $T_3 = 185.4$°C. Then the temperatures of the superheated steam after superheater SH1 and SH2 are determined as follows:

$$\Delta T_{\mathrm{SH2}} = T_0 - T_{\mathrm{SH2}}. \tag{1}$$

The saturation temperature of the heating steam and the pressure of the first extraction are:

$$T_{\mathrm{s,SH1}} = T_1 = T_{\mathrm{SH1}} + \Delta T_{\mathrm{SH1}};\ P_1 = f(T_{\mathrm{s,SH1}}). \tag{2}$$

The pressure of the first extraction is also the pressure of the heating steam in superheater SH1.

To determine the enthalpy at the end of the theoretical and actual expansion processes, it is necessary to determine the entropy at the inlet to the HIPT or LPT section as:

$$s_j = f(P_j, h_j), \tag{3}$$

where j is the extraction number.

The enthalpy at the end of the theoretical process can be found from:

$$h_{jt} = f(P_j, s_{j-1}). \tag{4}$$

The enthalpy at the end of the actual steam expansion process in the cylinder can be determined from:

$$h_j = h_{j-1} - \eta_{0i}\,(h_{j-1} - h_{jt}). \tag{5}$$

Further, the parameters of the steam expansion process in the HIPT and LPT are calculated using Eqs. (3), (4), and (5).

The enthalpies of the main condensate after the condenser, the LPH, HPH, and the feedwater are determined as functions:

$$T_{sj} = f(P_j); h_{sj} = f(T_{sj}); t_{fw} = t_{sj} - \theta; h_{fw} = f(P_{fw}, t_{fw}). \tag{6}$$

where t_{sj}– saturation temperature at the extraction pressure; h_{sj} – enthalpy of saturated water; t_{fw}– feedwater temperature after the regenerative heater; θ – feedwater terminal temperature difference relative to the saturation temperature of the heating steam; h_{fw}– feedwater enthalpy.

Further calculations of the cycle configuration were carried out to determine the steam extraction parameters in the regenerative system that ensure the maximum efficiency of the K-1000-60/1500-2 steam turbine unit. It should be noted that, during the variation of steam extraction parameters, the division of turbine sections into stages was not taken into account.

The steam extraction pressures were varied within the following ranges: $P_1 = 2.4$–3.5 MPa; $P_2 = 1.3$–1.9 MPa; $P_4 = 0.45$–0.8 MPa.

The minimum pressure value $P_1 = 2.4$ MPa was selected based on the condition that $T_{\mathrm{s,SH1}}$ should not be lower than 206 °C in order to ensure a uniform distribution of heating between SH1 and SH2.

The temperatures T_{SH2} and T_{SH1} were determined using Eqs. (1) and (2) at:

$$\Delta T_{\mathrm{SH2}} = 10°\mathrm{C}; \Delta T_{\mathrm{SH1}} = 15°\mathrm{C}.$$

The extraction pressures of the LPT were specified as follows:

$$P_6 = 0.075\ \mathrm{MPa}; P_7 = 0.015\ \mathrm{MPa}.$$

We obtained the dependence of STU efficiency on steam extraction pressure in the HIPT (Fig. 2).

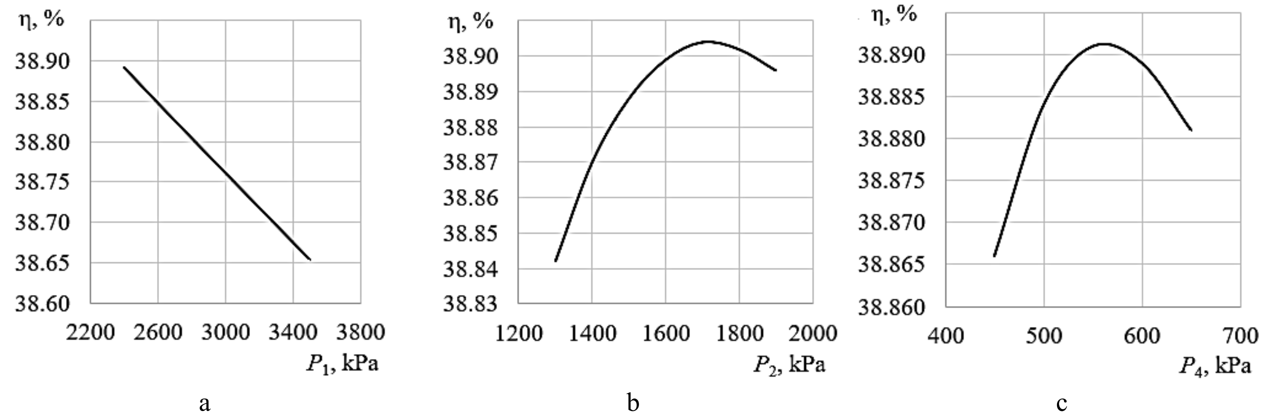

Figure 2. Dependence of the STU efficiency on steam extraction pressures in the HIPT:
a –P_1 at $P_2 = 1.7$ MPa and $P_4 = 0.55$ MPa; b – P_2 at $P_1 = 2.4$ MPa and $P_4 = 0.55$ MPa;
c – P_4 at $P_1 = 2.4$ MPa and $P_2 = 1.7$ MPa

Figure 2 shows that the highest efficiency values are observed at:

$$P_1 = 2.4 \text{ MPa}; P_2 = 1.7 \text{ MPa}; P_4 = 0.55 \text{ MPa}.$$

For these parameters corresponding to the maximum efficiency, an analysis of the LPT extraction parameters was carried out within the ranges presented on Fig. 3.

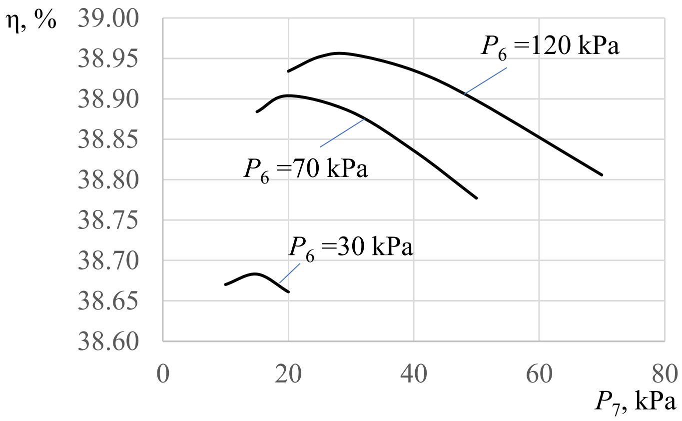

Figure 3. Dependence of the STU efficiency on P_6 and P_7

The results demonstrate that the maximum efficiency values are achieved at: $P_6 = 120$ kPa, $P_7 = 30$ kPa; $P_6 = 70$ kPa, $P_7 = 20$ kPa; $P_6 = 30$ kPa, $P_7 = 15$ kPa.

4.3 DETERMINATION OF OPTIMAL STEAM EXTRACTION PARAMETERS FOR THE AP1000-BASED STEAM TURBINE UNIT CONSIDERING THE NUMBER OF TURBINE STAGES

Several AP1000-based STU options with different numbers of turbine stages were considered. The calculations used modern numerical methods for gas-dynamic analysis and flow-part design of steam turbines [21–22].

Two options are given as an example.

In the first option, the number of stages in the high-pressure turbine part (HIPT, before the separator) was set to 6. In the first option, the number of stages in the high-pressure turbine part (HIPT, before the separator) was selected as 6 stages. The intermediate-pressure turbine part (HIPT, after the separator) had 3 stages. The number of cylinders/steam flow parts was 1. The LPT had 5 stages, and the number of cylinders/steam flow parts was 2.

In the second option, the high-pressure turbine had 4 stages. The intermediate-pressure turbine had 2 stages. The LPT had 6 stages.

Tables 1 and 2 present the steam pressures after each stage for both options.

The energy characteristics of the first option are as follows: the heat transferred to the steam in the steam generator is $Q_h = 3416$ MW; the gross electric power output is $N_e = 1330$ MW; and the internal efficiency of the STU cycle is η = 38.93 %.

Table 1. Steam pressure between turbine stages and steam mass flow rate, Option 1

Steam extraction number	Axial clearance between stages No. – No	Pressure in the axial clearance, MPa	Steam mass flow rate in the extraction, kg/s
High-pressure turbine part of the HIPT – 6 stages			
	1-2	4.214	
	2-3	3.182	
1	3-4	2.405	131
2	4-5	1.819	84
	5-6	1.377	
3	Steam exhaust	1.133	74
Intermediate-pressure turbine part of the HIPT – 3 stages			
	1-2	0.760	
4	2-3	0.548	35
5	Steam exhaust	0.372	59
2 LPT– 5 stages			
6	1-2	0.166	89
	2-3	0.075	
7	3-4	0.034	65
	4-5	0.015	

Table 2. Steam pressure between turbine stages and steam mass flow rate, Option 2

Steam extraction number	Axial clearance between stages No. – No	Pressure in the axial clearance, MPa	Steam mass flow rate in the extraction, kg/s
High-pressure turbine part of the HIPT – 4 stages			
	1-2	3.578	
1	2-3	2.296	172
2	3-4	1.477	37
3	Steam exhaust	1.133	68
Intermediate-pressure turbine part of the HIPT – 2 stages			
4	1-2	0.586	41
5	Steam exhaust	0.372	83
2 LPT– 6 stages			
	1-2	0.207	
6	2-3	0.113	70
	3-4	0.060	
7	4-5	0.031	63
	5-6	0.015	

The energy characteristics of the second option are as follows: $Q_h = 3416$ MW; $N_e = 1331$ MW; and the internal efficiency of the STU cycle is $\eta = 38.96$ %.

As can be seen, both options demonstrate high efficiency. To finalize the cycle configuration, an exergy analysis of the proposed STU configuration options is necessary.

5. EXERGY ANALYSIS OF THE STU CYCLE CONFIGURATION FOR OPERATION WITH THE AP1000 NUCLEAR REACTOR

The analysis of power generation systems is of significant scientific interest and is essential for the efficient use of energy resources. The most common method for analyzing energy conversion systems is energy analysis, which is based on the first law of thermodynamics. However, this approach does not provide a complete assessment of system efficiency and losses. Therefore, a combined approach that accounts for both the first and second laws of thermodynamics is becoming increasingly widespread.

Exergy analysis, based on the second law of thermodynamics, allows a clear distinction between losses to the environment and internal process irreversibility. This method provides an effective assessment of equipment and processes within energy conversion chains. Process exergy is a measure of its efficiency or inefficiency and enables a better understanding of the mechanisms of energy losses.

The modern approach to process analysis is based on the exergy method, which provides a clear understanding of the process and allows the quantitative assessment of exergy destruction. The main objective of traditional thermodynamic analysis is the conservation of energy.

The mass, energy, and exergy balances for any control volume operating under steady-state conditions with a steady flow, in which changes in kinetic and potential energy are negligible, can be expressed as follows [23]:

$$\sum G_i = \sum G_o, \tag{7}$$

$$\sum_k Q_k + \sum_i (G_i h_i)_k = \sum_e (G_e h_e)_k + N_k, \tag{8}$$

$$\sum_k E_{Q,k} + \sum_i G_i e_i = \sum_j G_j e_j + N_k + E_{D,k,} \tag{9}$$

where i and j are indices corresponding to the inlet and outlet states, and k denotes a specific cycle component; $\dot{Q}$ and $\dot{N}$ are the thermal and mechanical energy flow rates; $\dot{G}$ is the mass flow rate of the working fluid; h is the enthalpy; $\dot{E}_D$ is the exergy loss during the process, or exergy destruction; $\dot{E}_Q$ is the exergy transferred through heat transfer at temperature T, defined as:

$$E_{Q,k} = \sum \left(1 - \frac{T_{amb}}{T}\right) Q_k, \tag{10}$$

where T_{amb} is the ambient temperature. The temperature was assumed to be 25 °C.

The specific flow exergy is determined by the following expression:

$$e_{i,k} = h_{i,k} - h_0 - T_{amb}\left(s_{i,k} - s_0\right), \tag{11}$$

where $s_{i,k}$ – the specific entropy; the subscript “0” denotes the ambient environment.

The exergy flow rate is obtained:

$$E_{i,k} = G_{i,k} e_{i,k}. \tag{12}$$

Using the fuel–product (F–P) concept definitions [23, 24], the fuel and product terms can be expressed through exergy flows.

The exergy balance for an individual component (k) is written as:

$$E_{F,k} = E_{P,k} + E_{D,k}. \tag{13}$$

where E_P is the exergy flow of the useful product, and E_F is the fuel exergy required to obtain it.

Thus, the exergy efficiency can be determined:

$$\eta_{ex,k} = \frac{E_{P,k}}{E_{F,k}} = 1 - \frac{E_{D,k}}{E_{F,k}}. \tag{14}$$

The exergy efficiency of the cycle is calculated using the following equation:

$$\eta_{ex} = 1 - \frac{\sum E_{D,k}}{Q_h}. \tag{15}$$

The exergy flow into fuel and product is decomposed using the *F-P* method [23, 24], where fuel is considered as the decrease in exergy, while product is the increase in exergy within the component. The exergy E_i is determined using Eq. (12), where *G* is the total steam flow rate leaving the reactor heat exchanger.

For example, the exergy of the high-pressure part (h-p) of the HIPT is defined as the difference in exergy at the input and output, taking into account the change in steam mass:

$$E_{F,\text{h-p HIPT}} = (1-y_1)\cdot(E_0 - E_1) + (1 - y_1 - y_2 - \alpha_1)\cdot(E_1 - E_2) + (1 - y_1 - y_2 - \alpha_1 - \alpha_2)\cdot(E_2 - E_3),$$

where: α_i– fraction of steam extracted to the LPHs and HPHs; γ_i– fraction of steam extracted to the steam SHs.

The exergy product is the power of the high-pressure part of the HIPT. The difficulty lies in separating the fuel and product flows within the deaerator. Fuel exergy is defined as the sum of all incoming flows, and product is defined as the outgoing flow. Table 3 shows the decomposition of exergy flows into fuel and product flows.

Table 3. Decomposition of exergy flows into fuel and product of the STU (Fig. 1).

Element Name	$E_{F,k}$	$E_{P,k}$
NR	Q_h	$E_{NR} - E_{20}$
SV	E_{NR}	E_0
h-p HIPT	$(1–y_1)\cdot(E_0– E_1)+(1–y_1– y_2–\alpha_1)\cdot(E_1– E_2)+$ $+(1–y_1– y_2–\alpha_1–\alpha_2)\cdot(E_2 – E_3)$	$N_{\text{h-p HIPT}}= G\,((1–y_1)\cdot(h_0– h_1)+ (1–y_1– y_2–\alpha_1)\cdot(h_1– h_2)+(1–y_1– y_2–\alpha_1–\alpha_2)\cdot(h_2 – h_3))$
S	$(1–y_1– y_2–\alpha_1–\alpha_2–\alpha_3)\cdot E_3 – \alpha_S E_{Ss}$	$(1–y_1– y_2–\alpha_1–\alpha_2–\alpha_3–\alpha_s)\cdot E_S$
SH1	$y_2\,(E_1–E_{1s})$	$(1–y_1– y_2–\alpha_1–\alpha_2–\alpha_3–\alpha_S)\cdot(E_{SH1}– E_S)$
SH2	$y_1\,(E_0–E_{0s})$	$(1–y_1– y_2–\alpha_1–\alpha_2–\alpha_3–\alpha_S)\cdot(E_{SH2}– E_{SH1})$
i-p HIPT	$(1–y_1 – y_2 –\alpha_1–\alpha_2–\alpha_3–\alpha_s– \alpha_T)\cdot(E_{SH2}–E_4)+(1–y_1– y_2–\alpha_1–\alpha_2–\alpha_3–\alpha_c – \alpha_T–\alpha_4)\cdot(E_4– E_5)$	$N_{\text{i-p HIPT}} = G\,((1–y_1 – y_2 –\alpha_1–\alpha_2–\alpha_3–\alpha_s– \alpha_{18})\cdot(h_{SH2\text{-}4} – h_4)+ (1–y_1 – y_2 –\alpha_1–\alpha_2–\alpha_3–\alpha_c – \alpha_T– \alpha_4)\cdot(h_4 – h_5))$
LPT	$(1–y_1– y_2–\alpha_1–\alpha_2–\alpha_3–\alpha_c– \alpha_{18}– \alpha_4– \alpha_5)\cdot(E_5 – E_6)+ (1–y_1– y_2–\alpha_1–\alpha_2–\alpha_3–\alpha_c– \alpha_T–\alpha_4– \alpha_5–\alpha_6)\cdot(E_6 – E_7)+ (1–y_1– y_2–\alpha_1–\alpha_2–\alpha_3–\alpha_c– \alpha_T– \alpha_4– \alpha_5–\alpha_6– \alpha_7)\cdot(E_7 – E_8)$	$N_{LPT} = G\,(1–y_1– y_2–\alpha_1–\alpha_2–\alpha_3–\alpha_c– \alpha_{18}– \alpha_4– \alpha_5)\cdot(h_{5\text{-}6} – h_6)+ (1–y_1– y_2–\alpha_1–\alpha_2–\alpha_3–\alpha_c– \alpha_{18}– \alpha_4– \alpha_5–\alpha_6)\cdot(h_6 – h_7)+ (1–y_1– y_2–\alpha_1–\alpha_2–\alpha_3–\alpha_c– \alpha_T– \alpha_4– \alpha_5–\alpha_6– \alpha_7)\cdot(h_7 – h_8)$
C	$(1–y_1– y_2–\alpha_1–\alpha_2–\alpha_3–\alpha_c– \alpha_T– \alpha_4– \alpha_5 –\alpha_6– \alpha_7 –\alpha_T)\cdot(E_8– E_{10})$	E_{Q0} (10)
CP	$N_{CP}= \dot{G}\,(1–y_1– y_2–\alpha_1–\alpha_2–\alpha_3–\alpha_c–\alpha_4– \alpha_5 –\alpha_6– \alpha_7–\alpha_T)\cdot(h_{11} – h_{10})$	$(1–y_1– y_2–\alpha_1–\alpha_2–\alpha_3–\alpha_c–\alpha_4– \alpha_5 –\alpha_6– \alpha_7–\alpha_T)\cdot(E_{11} – E_{10})$
LPH1	$\alpha_7\cdot(E_7– E_{7s})+ \alpha_6\cdot E_{6s}$	$(1–y_1– y_2–\alpha_1–\alpha_2–\alpha_3–\alpha_c–\alpha_4– \alpha_5–\alpha_T)\cdot E_{12} – (1–y_1– y_2–\alpha_1–\alpha_2–\alpha_3–\alpha_c–\alpha_4– \alpha_5 – \alpha_6– \alpha_7–\alpha_T)\cdot E_{11}$
LPH2	$\alpha_6\cdot(E_6– E_{6s})$	$(1–y_1– y_2–\alpha_1–\alpha_2–\alpha_3–\alpha_c–\alpha_4– \alpha_5–\alpha_T)\cdot(E_{13} – E_{12})$
LPH3	$\alpha_5\cdot(E_5– E_{5s})+ \alpha_4\cdot E_{4s}$	$(1–y_1– y_2–\alpha_1–\alpha_2–\alpha_3–\alpha_s–\alpha_T)\cdot E_{14} – (1–y_1– y_2–\alpha_1–\alpha_2–\alpha_3–\alpha_c–\alpha_4– \alpha_5–\alpha_T)\cdot E_{13}$
LPH4	$\alpha_4\cdot(E_4– E_{4s})+ \alpha_T\cdot E_{Ts}$	$(1–y_1– y_2–\alpha_1–\alpha_2–\alpha_3–\alpha_s)\cdot E_{15} – (1–y_1– y_2–\alpha_1–\alpha_2–\alpha_3–\alpha_s–\alpha_T)\cdot E_{14}$
D	$\alpha_3\cdot E_3 + \alpha_s\cdot E_S +(1–y_1–y_2–\alpha_1–\alpha_2–\alpha_3–\alpha_s)\cdot E_{15} + (\alpha_1+ y_1+ \alpha_2+ y_2)\cdot E_{2s}$	E_{16}
T and TH	$\alpha_T\cdot(E_T– E_{Ts})$	$N_T= G\,\alpha_T\cdot(h_T– h_{21})$
FP	N_{FP}	$E_{17} – E_{16}$
HPH1	$\alpha_2\cdot(E_2 – E_{2s})+ y_2\,E_{1s} + (\alpha_1 + y_1)\,E_{1s}$	$E_{19}–E_{17}$
HPH2	$\alpha_1\cdot(E_1 – E_{1s})+ y_1\,E_{0s}$	$E_{20} – E_{19}$
EG	$N_e = (N_{\text{h-p HIPT}} + N_{\text{i-p HIPT}} + N_{LPT}) – (N_{CP} + N_{FP})$	$N_{EG}= N_e\cdot\eta_{EG}$, where η_{EG}– efficiency of an electric generator

Figure 4 shows the destruction of exergy in the elements of the STU. The exergy destruction in the nuclear reactor (NR) is not shown on Fig. 4, since it accounts for approximately 90% of the total exergy destruction in the STU. Figure 5 shows the exergy efficiency of each element.

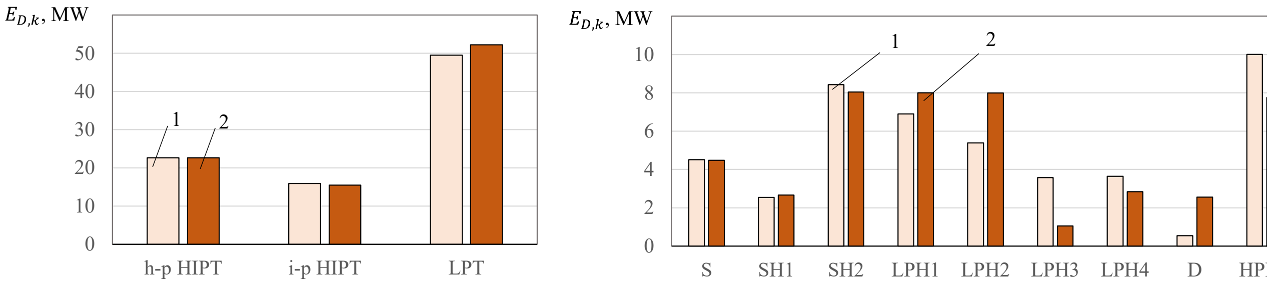

a b

Figure 4. Destruction of exergy in the elements of the STU

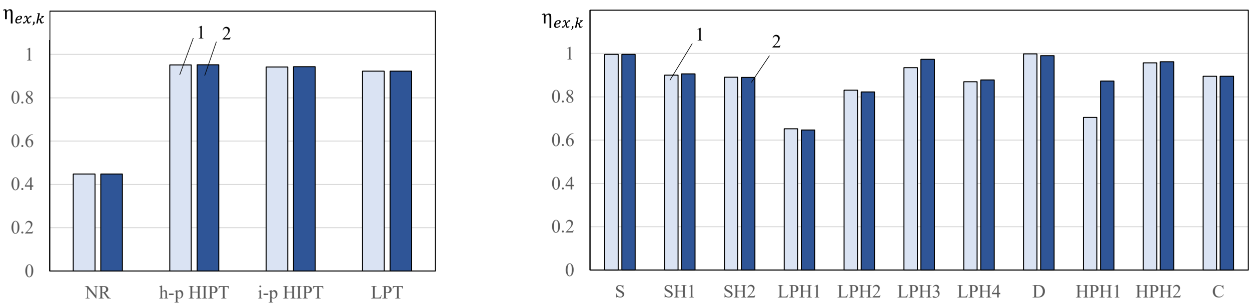

a b

Figure 5. Exergy efficiencies of the STU elements

Figure 4a shows that exergy destruction is highest in the low-pressure turbine section. In the second option, exergy destruction in the LPT is 3 MW higher (Fig. 4a). However, the exergy efficiency of the low-pressure turbine is the same for both variants and equals 0.92. (Fig. 5a).

Figure 4b shows that the highest exergy destruction among the regenerative heaters occurs in HPH1. For the second option, it is lower by 2.3 MW. At the same time, Fig. 5b shows that HPH1 efficiency in the second option is higher by 0.17.

Figure 4 also shows that when exergy destruction decreases in some components of the second option, it increases in others. As a result, the total exergy destruction of the second option is lower by only 0.5 MW. This indicates that both options demonstrate high exergy efficiency.

For further analysis, it is necessary to evaluate the mass-dimensional characteristics. Table 4 presents some geometric characteristics of the turbine flow paths.

Table 4. Axial dimension of the turbine flow paths

Turbine parts	Number of stages	Axial dimension, m
Option 1		
High-pressure turbine part of the HIPT	6	2.195
Intermediate-pressure turbine part of the HIPT	3	1.841
LPT	5	3.237
Option 2		
High-pressure turbine part of the HIPT	4	1.744
Intermediate-pressure turbine part of the HIPT	2	1.092
LPT	6	3.598

Table 4 shows that the largest axial dimension is observed in the LPT of the second option, while the total number of stages is lower by 2 stages.

The final decision can be made based on a techno-economic analysis.

6. DISCUSSION

The obtained results demonstrate that the proposed AP1000-based steam turbine unit provides high thermodynamic and exergy performance while maintaining a relatively compact turbine configuration. The internal cycle efficiency of both investigated options exceeds 38.9 %, which corresponds to the performance level of modern saturated-steam nuclear power units with Generation III+ reactors. The small difference in efficiency between the investigated options indicates that the redistribution of turbine stages mainly affects the distribution of thermodynamic losses within the cycle rather than the overall cycle efficiency.

The performed exergy analysis showed that the largest exergy destruction occurs in the low-pressure turbine section. This is primarily associated with steam moisture formation during the final stages of expansion and with significant irreversible losses caused by large volumetric steam flow rates at low pressures. Similar tendencies are reported in studies devoted to exergy analysis of steam turbine units for nuclear power plants and saturated-steam cycles.

At the same time, the redistribution of stages between the high-, intermediate-, and low-pressure turbine sections changes the local exergy destruction in individual components. In the second option, the exergy destruction in the low-pressure turbine section increases, whereas the exergy destruction in some regenerative heaters decreases. As a result, the total exergy destruction differs only slightly between the investigated configurations. This indicates that both options are thermodynamically balanced and characterized by high exergy efficiency.

The obtained results also show that increasing the number of stages in the low-pressure turbine section leads to an increase in the axial dimensions of the turbine flow path. However, the second configuration simultaneously reduces the total number of turbine stages and simplifies the overall structure of the steam turbine unit. Such an approach may reduce the metal consumption, simplify maintenance, and decrease the dimensions of the turbine hall.

Compared with conventional steam turbine units designed for VVER-1000 reactors, the proposed configuration is better adapted to the thermodynamic parameters of the AP1000 saturated steam cycle. The use of a combined single-flow high- and intermediate-pressure turbine, together with a two-stage reheating system, enables improved distribution of thermal and exergy losses within the cycle.

The obtained results confirm that exergy analysis is an effective tool for evaluating the thermodynamic perfection of nuclear steam turbine cycles and for identifying the components with the highest irreversible losses. The developed approaches may be used to further optimize AP1000-based steam turbine units, including detailed 3D flow-path optimization, moisture reduction in the low-pressure stages, and further improvement of the regenerative feedwater heating system.

7. CONCLUSIONS

1. A review of steam turbine units for nuclear power plants was carried out, and the K-1000-60/1500-2 turbine was selected as the baseline configuration for operation with the AP1000 nuclear reactor. Based on this turbine, a new cycle configuration of the steam turbine unit was developed. The proposed configuration includes a combined single-flow high- and intermediate-pressure turbine, two low-pressure turbines, a steam separator, and a two-stage steam reheating system.

2. Thermodynamic modeling of the AP1000-based steam turbine unit was performed. Optimal steam extraction pressures ensuring the maximum cycle efficiency were determined. The obtained results showed that the highest efficiency values correspond to the extraction pressures $P_1 = 2.4$ MPa, $P_2 = 1.7$ MPa, and $P_4 = 0.55$ MPa for the HIPT extraction system. For the LPT extraction system, the optimal parameters correspond to $P_6 = 120$ kPa and $P_7 = 30$ kPa.

3. Several options of the cycle configuration that consider different numbers of turbine stages were developed and analyzed. Two main configurations were investigated. The first option includes a 6-stage high-pressure part, a 3-stage intermediate-pressure part, and a 5-stage low-pressure turbine. The second option includes a 4-stage high-pressure part, a 2-stage intermediate-pressure part, and a 6-stage low-pressure turbine. Both options demonstrated high thermodynamic performance, with internal cycle efficiencies of 38.93% and 38.96%, respectively. The obtained efficiency values are comparable to those of modern saturated-steam nuclear power units reported in the literature, where the cycle efficiency typically ranges from 37–39% [25, 26].

4. A full exergy analysis of the steam turbine unit was carried out. The exergy destruction in the main elements of the cycle configuration was determined using the fuel–product approach. The results showed that the largest exergy destruction occurs in the low-pressure turbine section. At the same time, the redistribution of exergy destruction between the components of the two investigated options results in only a small difference in the total exergy destruction. Both configurations demonstrated high exergy efficiency characteristics.

5. The analysis of the geometric characteristics of the turbine flow paths showed that the second option has larger axial dimensions in the low-pressure turbine section despite the lower total number of stages.

6. The obtained results can be used for further development and optimization of AP1000-based steam turbine units. The final selection of the cycle configuration should be based on a comprehensive thermodynamic, exergy, and economic analysis.

Acknowledgements

This work was carried out within the framework of the research project "Development of a highly efficient and competitive steam turbine plant for promising power units of Ukrainian NPPs with AP1000 nuclear reactors. Section 1. Power generating steam turbine plant. Stage I "Analysis of existing thermal schemes of steam turbine plants and their loading modes for promising power units of Ukrainian NPPs with AP1000 nuclear reactors" with state registration number 0125U001698.

ORCID

Andrii V. Rusanov, https://orcid.org/0000-0002-9957-8974, **Andrii O. Kostikov,** https://orcid.org/0000-0001-6076-1942, **Viktoriia O. Tarasova,** https://orcid.org/0000-0003-3252-7619, **Roman A. Rusanov**, https://orcid.org/0000-0003-2930-2574, **Marina O. Chugay,** https://orcid.org/0000-0002-0696-4527, **Maksym V. Lytvynenko,** https://orcid.org/0000-0003-2805-234X

REFERENCES

[1] Westinghouse Electric Company. AP1000® Plant Overview. Available at: https://westinghousenuclear.com/energy-systems/ap1000-pwr/overview
[2] W.E. Cummins, M.M. Corletti, and T.L. Schulz, "Westinghouse AP1000 Advanced Passive Plant," in: *Proceedings of ICAPP'03*, (Cordoba, Spain, 2003). Paper 3235. Available at: http://large.stanford.edu/courses/2022/ph241/beskind1/docs/cummins-may03.pdf
[3] AP1000 Design Control Document Rev. 16 – Tier 2 Chapter 1 – Introduction and General Description of the Plant – Section 1.9 Compliance with Regulatory Criteria. Available at: https://www.nrc.gov/reactors/new-reactors/design-cert/ap1000/dcd.html
[4] On Siting, Design and Construction of Energy Blocks N3 and N4 of the Khmelnitsky Nuclear Power Plant: Law of Ukraine No. 5217-VI of September 6, 2012. Database "Legislation of Ukraine". Verkhovna Rada of Ukraine. Available at: https://zakon.rada.gov.ua/laws/show/en/5217-17?utm_source=chatgpt.com#Text
[5] T.V. Petik, and H.P. Lisiuk, "Automatic system of regulation of water level in the steam generator of the 1000 MW nuclear power plant," Scientific notes of Taurida National V.I. Vernadsky University, series «Technical Sciences», **30**(69), Part 2, No. 3, 7–13 (2019). (in Ukrainian). https://doi.org/10.32838/2663-5941/2019.3-2/02
[6] O.M. Uss, S.T. Patsiuk, O.V. Panchenko, O.V. Shavlaklov, and D.Kh. Kharlampidi, "New Generation 'Block-Modular' Condenser for K-1000-60/1500-2 Turbine Units in Zaporozhskaya NPP," J. of Mech. Eng. **21**(1), 4-10 (2018). https://doi.org/10.15407/pmach2018.01.004
[7] O.V. Shavlakov, M.O. Feofentov, O.V. Panchenko, O.G. Kasatkin, O.M. Uss, S.T. Patsyuk, O.V. Vavilov, *et al.*, *Development and implementation of condensers for steam turbines of nuclear power plants*, (FOP Panov A.M., Kharkiv, 2018). (in Ukrainian)
[8] New nuclear reactors: Generic Design Assessment. Report by the Office for Nuclear Regulation on the Generic Design Assessment of new nuclear reactor designs. 2011. Available at: https://www.onr.org.uk/media/sbkc5dng/ap1000-onr-gda-sr-11-002-rev-0.pdf
[9] S.A. Olatubosun, A. Ayodeji, and M.A. Amidu, "Safety assessment of AP1000: Common transients and their analysis," Nuclear Engineering and Design, **375**, 111100 (2021). https://doi.org/10.1016/j.nucengdes.2021.111100
[10] L.T. Borges, D.G. Rodríguez, C.J.C.M.R. da Cunha, J. de Lima Bezerra, and C.A.B. de Oliveira Lira, CFD Analysis of the AP1000 Reactor Pressure Vessel under Normal Operating Conditions. 2024. Available at: https://sencir.nuclear.ufmg.br/wp-content/uploads/2024/11/956358.pdf
[11] Idaho National Laboratory. Opportunities for AP1000 Deployment at Existing and Planned Nuclear Sites. 2024. Available at: https://inldigitallibrary.inl.gov/sites/STI/STI/Sort_128167.pdf.
[12] X. Niu, J. Liu, Z. Dong, J. Wei, and W. Zhou, "Research on Neutronics Safety Parameters of the AP1000 Nuclear Reactor under Different Conditions," Energies, **16**, 7549 (2023). https://doi.org/10.3390/en16227549
[13] Z. Winfried, B. Nadine, A. Alexander, and V. Kiril, "Sensitivities of delayed neutron fractions in the framework of SCALE 6.2," Annals of Nuclear Energy, **153**, 108068 (2021). https://doi.org/10.1016/j.anucene.2020.108068
[14] M. Rahgoshay, and O. Noori-Kalkhoran, "Calculation of control rod worth and temperature reactivity coefficient of fuel and coolant with burn-up changes for VVRS-2 MWth nuclear reactor," Nuclear Engineering and Design, **256**, 322–331 (2013). https://doi.org/10.1016/j.nucengdes.2012.08.033
[15] H. Mazrou, D. Lababsa, and O. Mokhtari, "Assessment of the safety impact caused by the variations of the critical position of control rods and by the presence of an in-core flux trap on the power peaking factors in an MTR-type research reactor," Nuclear Engineering and Design, **414**, 112553 (2023). https://doi.org/10.1016/j.nucengdes.2023.112553
[16] A. Kluba, and R. Field, "Optimization and Exergy Analysis of Nuclear Heat Storage and Recovery," Energies, **12**(21), 4205 (2019). https://doi.org/10.3390/en12214205
[17] J.Y. Heo, J.H. Park, Y.J. Chae, S.H. Oh, S.Y. Lee, J.Y. Lee, N. Gnanapragasam, *et al.*, "Evaluation of various large-scale energy storage technologies for flexible operation of existing pressurized water reactors," Nuclear Engineering and Technology, **53**(8), 2427–2444 (2021). https://doi.org/10.1016/j.net.2021.02.023.
[18] W.M. Conlon, and Ch.W. Forsberg, "Storage-Coupled Nuclear Combined Cycle," ASME Open Journal of Engineering, **1**, 015001-1 (2022). https://doi.org/10.1115/1.4055277
[19] A.V. Rusanov, A.O. Kostikov, V.O. Tarasova, R.A. Rusanov, and S.P. Tretiak, "The concept of creating a maneuverable powerplant based on a small modular reactor." Naukovyi Visnyk Natsionalnoho Hirnychoho Universytetu, (5), 37–44 (2024). https://doi.org/10.33271/nvngu/2024-5/037
[20] M.A. Darwish, F.M. Al Awadhi, and A.O. Bin Amer, "Combining the nuclear power plant steam cycle with gas turbines," Energy, **35**, 4562–4571 (2010). https://doi.org/10.1016/j.energy.2010.04.031
[21] R. Rusanov, A. Rusanov, and M. Chugay, "Analysis of the Influence of Operational and Geometrical Characteristics on the Efficiency of Axial Turbine Stage Profile Cascades," Science and Innovation, **21**(2), 73–87 (2025). https://doi.org/10.15407/scine21.02.073
[22] A. Rusanov, R. Rusanov, P. Klonowicz, P. Lampart, G. Żywica, and A. Borsukiewicz, "Development and experimental validation of real fluid models for CFD calculation of ORC and steam turbine flows," Materials, **14**(22), 6879 (2021). https://doi.org/10.3390/ma14226879
[23] G. Tsatsaronis, "The future of exergy-based methods," Energy, **302**, 131881 (2024). https://doi.org/10.1016/j.energy.2024.131881

[24] D. Kharlampidi, V. Tarasova, M. Kuznetsov, and E. Voytenko, "Thermodynamic analysis of air-compression refrigerating machine based on the exergy cost theory," Eastern-European Journal of Enterprise Technologies, **5**(8(89)), 30–38 (2017). https://doi.org/10.15587/1729-4061.2017.112113

[25] A. Ohji, and M. Haraguchi, "2 - Steam turbine cycles and cycle design optimization: The Rankine cycle, thermal power cycles, and IGCC power plants," Advances in Steam Turbines for Modern Power Plants*,* 11–40 (2017). https://doi.org/10.1016/B978-0-08-100314-5.00002-6

[26] V. Solovey, M. Zipunnikov, and R. Rusanov, "Increasing the manoeuvrability of power units of the thermal power plants due to applying the hydrogen-oxygen systems," J. Phys. Energy, **5**, 014012 (2023). https://doi.org/10.1088/2515-7655/aca9ff

ТЕРМОДИНАМІЧНИЙ ТА ЕКСЕРГЕТИЧНИЙ АНАЛІЗ ПАРОТУРБІННОЇ УСТАНОВКИ НА БАЗІ AP1000 З ОПТИМІЗОВАНОЮ КОНФІГУРАЦІЄЮ ЦИКЛУ

Андрій В. Русанов[1], Андрій О. Костіков[1], Вікторія О. Тарасова[1], Роман А. Русанов[1], Марина О. Чугай[1], Максим В. Литвиненко[2]

[1]Інститут енергетичних машин і систем ім. А.М. Підгорного Національної академії наук України, вул. Комунальників, 2/10, м. Харків, 61046, Україна

[2]Інститут гідродинамічних машин Польської академії наук, вул. Фішера, 14, м. Гданськ, 80-231, Польща

З огляду на стратегічну важливість модернізації ядерної енергетики України у статті наведено результати дослідження з розроблення та аналізу термодинамічного циклу та структури теплової схеми паротурбінної установки (ПТУ), призначеної для роботи з ядерним реактором AP1000. За базову було обрано теплову схему турбоустановки К-1000-60/1500-2. На її основі запропоновано нову конфігурацію ПТУ, що включає комбінований однотечійний циліндр високого та середнього тиску (ЦВСТ), два циліндри низького тиску (ЦНТ), сепаратор пари та двоступеневу систему проміжного перегріву пари. Для оцінювання впливу тисків відборів пари, параметрів регенеративного підігріву живильної води та розподілу ступенів турбіни на показники циклу було проведено термодинамічний та ексергетичний аналіз запропонованих конфігурацій ПТУ. Чисельне моделювання та розрахунки проточної частини секцій турбіни виконано із застосуванням сучасних методів газодинамічного проєктування. Результати показали, що оптимальний вибір параметрів відборів пари та умов проміжного перегріву суттєво підвищує ефективність циклу. Максимальний внутрішній ККД циклу ПТУ досяг 38,96 %. Ексергетичний аналіз продемонстрував, що найбільші втрати ексергії спостерігаються в циліндрі низького тиску, водночас обидві досліджувані конфігурації характеризуються високою ексергетичною ефективністю. Також проведено порівняльний аналіз компонування ступенів та осьових розмірів проточних частин турбіни. Розроблені підходи можуть бути застосовані під час проєктування та оптимізації паротурбінних установок нового покоління для атомних електростанцій.

Ключові слова: *ядерна енергетика; AP1000; паротурбінна установка; термодинамічний аналіз; ексергетичний аналіз; регенеративний підігрів живильної води; атомна електростанція*